

**A vertical transport window of water vapor in the troposphere
over the Tibetan Plateau with implication for global [climate](#)
change**

**Xiangde Xu^{1,2}, Chan Sun^{1,2}, Deliang Chen³, Tianliang Zhao^{1*}, Jianjun Xu⁴,
Shengjun Zhang², Juan Li¹, Bin Chen², Yang Zhao², Hongxiong Xu², Lili Dong²,
Xiaoyun Sun¹, Yan Zhu¹**

¹ Nanjing University of Information Science and Technology, Nanjing 210044, China;

² State Key Laboratory of Disastrous Weather, China Academy of Meteorological
Sciences, Beijing, 100081, China;

³ Regional Climate Group, Department of Earth Sciences, University of Gothenburg,
Sweden;

⁴ South China Sea Institute of Marine Meteorology, Guangdong Ocean University,
Zhanjiang 524088, China

* Corresponding author. **Email:** tlzhao@nuist.edu.cn

Abstract

By using the multi-source data of meteorology over recent decades, this study discovered a summertime “hollow wet pool” in the troposphere with a center of high water vapor over Asian water tower (AWT) on the Tibetan Plateau (TP), where is featured by a vertical transport “window” in the troposphere. The water vapor transport in the upper troposphere extends from the vertical transport window over the TP with the significant connections among the Arctic, Antarctic and TP regions, highlighting an effect of TP’s vertical transport window of tropospheric vapor in the “hollow wet pool” on global change. The vertical transport window was built by the AWT’s thermal forcing in associated with the dynamic effect of the TP’s “hollow heat island”. Our study improve the understanding on the vapor transport over the TP with an important implication to global [climate](#) change.

34

35 1. Introduction

36 The Tibetan Plateau (TP) is the largest high terrain in the world, known as "the roof
37 of the world" with an averaged altitude over 4,000 meters. The rivers, such as the
38 Yangtze River, Yellow River, Lancang River and Ganges River, are all originated from
39 the TP, which is regarded as the "Asian Water Tower" (AWT) (Xu et al., 2008). The
40 Three-River-Source (Yangtze, Yellow, and Lancang Rivers) region (TRSR) in the eastern
41 TP is the core area of the AWT (Xu et al., 2014). The observed "CISK-like mechanism"
42 is an important mechanism sustaining the atmospheric "water tower" over the AWT (Xu
43 et al., 2014). Connecting with the cloud and precipitation in the AWT, the plausible
44 hydrological cycles could be realized with the transport of water vapor from tropical
45 oceans up to the TP (Xu et al., 2014).

46

47 Water vapor plays an important role in global environment and climate changes
48 (Tian et al., 2009; Solomon et al., 2010). The ratio of strong convective clouds to total
49 clouds over the Tibetan Plateau (TP) is about 5 times to the global ratio, and the frequent
50 occurrences of strong convective clouds could be largely attributed to the TP's large
51 topography (Luo et al., 2011; Su et al., 2006). The water vapor in the ~~tropical~~ upper
52 troposphere is mainly originated from the tropical lower troposphere through vertical
53 transport ~~convective~~ transport and evaporation of convectively transported or in situ
54 produced cloud ices (Tian et al., 2004; James, et al., 2008). Water vapor was first lifted by
55 convection over the Bay of Bengal and the South China Sea and then transported
56 upwards the tropical tropopause layer via the monsoon anticyclonic circulations towards

Northwest India (Yanai, et al., 1973; Chen, et al., 2012). TP is a moisture sink in summer, having a net moisture convergence of 4 mm/day, where the convergences ~~were~~ enhanced from 1979 to 2018 (Feng and Zhou, 2012; Xu, et al., 2020). In general, Asian monsoon circulation provides an effective pathway for regional water vapor transport to the TP (Wang, et al., 2017). An important role of the anticyclone over the TP is verified in the exchange of water vapor between the troposphere and stratosphere (Garny, et al., 2016; Fu, et al., 2006). Many studies have been focused on the transport of water vapor into upper troposphere and lower stratosphere from the tropical oceans to the TP (Chen, et al., 2012; Wang, et al., 2017; Xie, et al., 2018; Randel, et al., 2013). However, ~~inadequate~~ ~~not enough~~ attention has been paid to the vertical transport of water vapor in the troposphere over the TP, especially in respect of the underlying mechanism and the consequences on global climate.

The following questions are ~~also~~ of great concern in the TP's vertical transport of water vapor study with implication for global change, for example, what is the ~~forcing~~ formation mechanism ~~forming on~~ the vertical transport window of water vapor in the troposphere on the TP? How is the ~~AWT's special column constructor built for the~~ vertical transport of water vapor in the TP-troposphere constructed with the special column of apparent heat source in the AWT over the TP? How is the global effect of the vertical transport window of water vapor in the troposphere on the TP? From the perspective of global atmospheric energy and water vapor exchanges, this study characterizes a window of water vapor vertical transport within the troposphere over the TP and the implication for global change.

2. Data and Methods

The daily meteorological data of cloud amount are provided by the meteorological observatories in the TP in the period of 1979 to 2016. The AIRS remote sensing products of water vapor [from 2003 to 2018](#) and the ECMWF-interim data of meteorology [from 1979 to 2018](#) are used in this study.

In this study, the inverse algorithm is used to calculate the apparent heat source Q_l , and the formula is as follows (Su et al., 2006) :

$$Q_1 = C_p \left[\frac{\partial T}{\partial t} + \vec{V} \cdot \nabla T + \left(\frac{p}{p_0} \right)^k \bar{\omega} \frac{\partial \theta}{\partial p} \right] \quad (1)$$

where T is air temperature; ω is the vertical velocity at the p coordinate, $P_0 = 1000$ hPa;

$k = R/C_p$; V is the horizontal wind vector; θ is the potential temperature.

Vertical integration of Q_l is expressed as:

$$\langle Q_1 \rangle = \frac{1}{g} \int_{p_t}^{p_s} Q_1 dp \quad (2)$$

where p_s is the surface air pressure, p_t is the top air pressure, here taken as 100hpa.

In order to analyze the relationship between water vapor source tracing and its channels in the atmospheric water cycle over the TP, the correlation vector calculation

was used to calculate the temporal and spatial variations of the water vapor transport channel. The expression is:

$$\vec{R}(x, y) = R_u(x, y)i + R_v(x, y)j \quad (3)$$

where $\vec{R}(x, y)$ represents the correlation vector in which $R_u(x, y)$ represents the correlation coefficients between ~~rainstorm or precipitation frequency~~ water vapor and the component of latitudinal water vapor flux qu , and $R_v(x, y)$ represents correlation coefficients between water vapor ~~rainstorm or precipitation frequency~~ and longitudinal water vapor flux components qv .

3. Results and discussion

3.1 The structures of vertical transport window of water vapor over the TP

With the use of satellite remote sensing ~~products~~productions from 2003 to 2016, the global distribution of the total water vapor from 500_hPa to 300_hPa in the troposphere was ~~calculated and~~ shown in Figures 1a. The results indicate that there is a high value center of ~~the~~ water vapor in the mid- and upper troposphere over the TP, extending southwards to the Bay of Bengal, India and Northern Southeast Asia. It is worth noting that the fraction of strong convective cloud to the total cloud ranges from 4.0 % to 21.0 % in the TP, ~~and the TP~~ during the summer season the thermal forcing of TP is dominated by the latent heat released by cloud and precipitation (Fu et al.,2006; Dessler et al.,2006; Gao et al.,2014). The intense mesoscale convective activity, which is represented with the low cloud fraction based on the cloud characteristics observed in the TP, and the "massive chimney effect" of huge cumulonimbus cloud drive the~~continue to~~

transport of atmospheric heat and water vapor to the upper troposphere(Fu et al.,2006; Xie et al.,2018) . Based on Chinese Third Tibetan Plateau Experiment-Observation of Boundary Layer and Troposphere (2014–2017), it is observed in the TP that the ~~mean~~ cloud-top height was averaged around 11.5 km (a.s.l.),~~and with~~ its maximum value exceeded 19 km (a.s.l.), and the mean cloud-base height was 6.88 km (a.s.l.) during the observation period, reflecting the TP's ~~the~~ deep convection in the troposphere and its impact on the upper troposphere.

3.2 Global effect of the vertical transport window over the TP

The vertical section of the correlation coefficients along the south-north direction between the low cloud cover on the TP and the global water vapor are presented in Figure 1b. The obviously upward movement of water vapor over the TP can be seen in Figures 2a. It could be noticed that there exists the structures similar with the massive chimney between the convective cloud and the water vapor on the TP (Figures 1b and 2a). Figures 2b and 2c show significant correlation between convective clouds over the AWT and the changes of global water vapor from 1979 to 2018. Significant correlations extend from the TP southward and northward in the upper troposphere. It is remarkable that the high correlation area exceeding the 95 % confidence level expand towards the polar regions of both the southern and the northern hemisphere (Figure 1b, 2b and 2c), ~~depictand-ing~~ the relation between the convective clouds and the global water vapor in the upper troposphere across the northern and southern hemispheres for an implication of the TP to global climate change~~could be depicted.~~

The distributions of high positive correlation coefficients between low cloud cover over the TP and the global the water vapor in the upper troposphere are calculated by ECMWF-interim reanalysis data (Figure 3a). It can be found that there is a region with highest values of correlation coefficients in the upper troposphere (500-hPa-300-hPa), covering a banded large area from the plateau ~~te~~across the lower latitude tropical zone to the polar regions, ~~which could~~indicateing the significant correlations between convective cloud activities on the TP and the global water vapor in the upper troposphere, especially in the polar region of the southern hemisphere area (Figure 3a), which could be reflected an importance of the thermal forcing of TP in global changes of water vapor.

The strong anticyclone in the upper troposphere over the southeastern TP takes a significant part in the upward transport of water vapor in the troposphere and stratosphere (Garny, et al., 2016;Fu, et al., 2006) . In order to understand the effect of the vertical transport window of troposphere over the TP on the global water vapor distribution from the perspective of the dynamic effect of anticyclone over the plateau driven by the heat sources, we presented the distributions of correlation coefficients between daily mean Q_1 in the TRSR and global water vapor flux in July from 2014 to 2016 at 300hPa (Figure 3b.) Driven by the heat source of the TP, the anticyclone is formed in the upper troposphere over the TP, which driven the water vapor transport form the TP not only to the surrounding area, but also extending to the north and south poles along the long-range transport channels (Figure 3b). This confirms the vertical transport window effect of the TP on global water vapor transport, especially over high-latitude regions such as the Arctic and Antarctic. To further verify the global transport pathways of water vapor from

the TP, we used the methods of composite analysis to characterize global distribution of water vapor transport fluxes at the 300hpa in the years to anomalously high and low Q1 over the AWT. The Asian monsoon anticyclone in the upper troposphere is often associated with deep convection in the troposphere(Garny, et al., 2016). Figure 3c shows that in years with higher Q₁, stronger anticyclone formed at the upper level (Figure 3b), which maintains the upward transport of water vapor to the upper troposphere, with strong transport of water vapor transport the arctic and antarctic (Figure 3c), confirming the impact of the vertical transport in the troposphere driven by heat released within AWT on global water vapor transport especially to the polar regions.

The Indian continent heats up in spring and summer, convection draws moisture northwards from the Bay of Bengal, Arabian Sea and Indian Ocean, leading to precipitation in the Himalayas and beyond (Yanai et al., 1973). In Figure 3db, it could be found that, driven by the strong apparent heat source, the water vapor flows from the lowwarm and wet water vapor flows on the Asian water tower (AWT) over the TP coming from the low latitude ocean could build a remarkable channel to the TP. The key entrance to the water vapor passage is just the intersection of the Himalayas on the southern slope of the TP. This region constitutes a special canyon pass in the plateau with deep valleys, making a perfect entrance zone for the oceanic warm-wet water flows (see the terrain distribution inserted in the lower right corner of Figure 3ed).

FLEXPART trajectory model (Stohl, et al., 2005;Reale,et al 2001; James, et al, 2004) was used to simulate the spatial and temporal changes of water vapor transport to the TRSR over the TP, driven with the ERA-Interim reanalysis data of meteorology with

horizontal resolution of $0.75^{\circ} \times 0.75^{\circ}$ in July 2009. In the FLEXPART particle diffusion model, the 80000 particles was released at the TRSR (90° - 102° E and 30° - 35° N). In Figure 3f, it can be found that the water vapor in the TRSR was traced to water vapor source on the tropical Indian Ocean. The water vapor from the central Indian Ocean in the southern hemisphere can be transported along the Somali jet flow through the Arabian Sea to the TP. The water vapor from the South China Sea and the Bay of Bengal was transported to the TP converging over the TRSR (Figure 3f), characterizing the water vapor transport channel from the southern hemispheric and low latitude oceans to the TP.

According to the correlation analysis of water vapor transport, the water vapor source of the AWT can also be traced back to the ocean surface water vapor source region with water vapor positive correlation extreme value region in the Chagos archipelago of the Central Indian Ocean near 10° S south of the equator (Figure 3d), revealing that the TP is the confluence area of across hemispherical water vapor from the southern Indian Ocean.

3.3 The transport window of water vapor driven by the AWT

Through the correlation analysis of the ~~column whole layer of~~ apparent heat source Q_1 over the ~~plateau region~~ TP as well as; the three-dimensional structure of vorticity and divergence, it can be found that the apparent heat source Q_1 in the TP ~~are is~~ an important forcing factor (Figure 4). The results show that the air heat island ~~over in~~ the AWT is located at 300-500 hPa in the upper troposphere, which is regarded as the high apparent heat (Figure 5). The Q_1 ~~is area~~ significantly related to the convective cloud and ~~its the~~ strong ascending movement (Figures ~~4a and 4d3b-3d~~), Figures 4b, 4c, 4e and 4f present

the correlations of the column apparent heat Q_1 in AWT with the divergence and vorticity fields over the TP, which can describe the effective "suction effect" with divergence (negative vorticity) at upper levels and convergence (positive vorticity) at lower levels in the troposphere. The Q_1 is significantly released in the convective clouds and the strong ascending movement, and there exists ~~also~~ a strong ~~high-level~~ anticyclone circulation in the upper troposphere ~~in~~ over the region of the AWT in the southeast of the plateau (Figure 3**db**). In addition, the lower troposphere is the center of strong convergence and strong vorticity ~~(Figure 4)~~. Figure 3g shows the difference of vapor transport flux and specific humidity at 500hPa in summer between anomalously high and low Q_1 . When the Q_1 in TRSR is anomalously high, large water vapor from the tropical oceans is transported across the Bay of Bengal and the Indian peninsula, and entered the TP from the southern edge, revealing the TP's thermal effect could make a strong vapor transport channel connecting the water vapor source in the low latitude tropical oceans.

All these results reveal the effective "pumping effect" of the vertical configuration with low-level cyclonic circulation and high-level divergence with anticyclone circulation ~~over the~~ ~~in~~ TP ~~(Figures 3b-3d)~~. The strong confluence effect building the vertical transport window of water vapor could be driven by the elevated heating on the TP in the ~~middle~~ troposphere with the water vapor flow, making a strong ~~warm wet~~ vapor transport ~~channel~~ connecting the water vapor source in the low latitude tropical ocean with the water vapor center over the core area of AWT over the TP. The water vapor transport connect from the vertical transport window over the TP and the Arctic, Antarctic regions in the upper troposphere, highlighting the effect of TP "hollow wet pool" on global climate change.

236

237 4. Conclusion

238 By using the multi-source data of meteorology over recent decades, this study
239 discovered a summertime “hollow wet pool” in the troposphere with a center of high
240 water vapor over AWT on the highly elevated TP, ~~where~~ich is featured by a vertical
241 transport window with the transport flux ~~columns~~ of water vapor in the troposphere.
242 Driven by the strong TP’s heat source, water vapor flows ~~are connected~~ the AWT over
243 the TP with the low-latitude oceans. Significant correlations exist between convective
244 activity on the TP and global water vapor in the upper-~~troposphere~~especially in the polar
245 ~~region of the southern hemisphere~~. The water vapor transport from the TP’s vertical
246 window in the upper troposphere extends from the TP globally towards the northern and
247 southern hemispheres ~~from the TP~~ with the significant connections among the three poles
248 of Arctic, Antarctic and TP regions, highlighting an effect of TP’s vertical transport
249 window of water vapor on global climate change. The vertical transport window was
250 built by the AWT’s thermal forcing in associated with the dynamic effect of the TP’s
251 “hollow heat island” as well as the effective "pumping effect" on vertical transport with
252 ~~of~~ low-level convergences with cyclonic circulation and high~~upper~~-level divergences
253 with anticyclone circulation in the troposphere over the TP.

254 Based on~~In~~ this observational study, a conceptual model of the comprehensive
255 relation of the TP region with the global energy and water cycles ~~under the thermal~~
256 ~~forcing in the core region of the AWT was~~is put forward for the vertical transport window
257 of vapor in the troposphere driven by the thermal forcing in the core region of the AWT
258 over the TP(Figure 65), where ~~the "core area" of AWT is the key entrance of the low-~~

~~latitude warm and moist air, and~~ the water vapor source was traced back to tropical
oceans and the Southern Hemisphere. The thermal heat-driving effect ~~on~~of the TP could
~~sustain~~contribute to the ~~maintenance of~~ vertical upward transport of the energy and water
vapor. The water cycle in the AWT clearly displayed the ~~connection~~ linkages of the
vertical transport window of water vapor in the troposphere over TP with the ~~warm-wet~~
vapor source in the ~~—~~tropical oceans and the southern Indian Ocean in the lower
troposphere and with the Arctic and Antarctic regions in the upper troposphere(Figure 5).
Our study depicted a comprehensive understanding on the vertical water vapor transport
in the atmosphere over the TP with an important implication to global climate change.

Data availability

ERA-Interim of ECMWF (
ECMWF, <https://apps.ecmwf.int/datasets/data/interim-full-moda/levtype=pl/>) reanalysis
daily and monthly data are part of the European Center for Medium-range Weather
Forecasts. AIRS Science Team/Joao Teixeira (2013), AIRS/Aqua L3 Daily Standard
Physical Retrieval (AIRS-only) 1 degree x 1 degree V006, Greenbelt, MD, USA,
Goddard Earth Sciences Data and Information Services Center (GES DISC),
Accessed: [Jan. 2019], 10.5067/Aqua/AIRS/DATA303. The low cloud data used in this
study are derived from the Data Sets of Surface Meteorological Elements in China
released by the National Meteorology Information Center, China Meteorological
Administration, which can be found at
<https://zenodo.org/record/5121157#.YPkRHqjitPY>

(<http://doi.org/10.5281/zenodo.5121157>).

Author Contributions

Xiangde Xu, Chan Sun and Tianliang Zhao conducted the study design. Deliang Chen, Jianjun Xu and Shengjun Zhang analysed the observational data. Juan Li, Bin Chen, Yang Zhao, Hongxiong Xu, Lili Dong, Xiaoyun Sun, and Yan Zhu assisted with data processing. Xiangde Xu, Chan Sun and Tianliang Zhao wrote [and revised](#) the manuscript. Xiangde Xu, Chan Sun, Tianliang Zhao, and Jianjun Xu were involved in the scientific interpretation and discussion. All authors provided commentary on the paper.

Acknowledgments

This study was supported by The Second Tibetan Plateau Scientific Expedition and Research (STEP) program (2019QZKK0105) and the Scientific and Technological Development Funds from Chinese Academy of Meteorological Sciences (2021KJ022 and 2021KJ013).

Financial support.

This study was supported by The Second Tibetan Plateau Scientific Expedition and Research (STEP) program (2019QZKK0105) and the Scientific and Technological Development Funds from Chinese Academy of Meteorological Sciences (2021KJ022 and 2021KJ013).

302

303 **Conflict of interest**

304 *Xiangde Xu, Chan Sun, Deliang Chen, Tianliang Zhao, Jianjun Xu, Shengjun Zhang,*
305 *Juan Li, Bin Chen, Yang Zhao, Hongxiong Xu, Lili Dong, Xiaoyun Sun and Yan Zhu*
306 *declare that they have no conflict of interest.*

307

308

309 **References**

310 Chen, B., Xu, X. D., Yang, S., and Zhao, T. L.(2012). Climatological perspectives of air transport from
311 atmospheric boundary layer to tropopause layer over Asian monsoon regions during boreal summer
312 inferred from Lagrangian approach. *Atmos. Chem. Phys.* ; 12: 5827-5839. [https://doi.org/10.5194/acp-](https://doi.org/10.5194/acp-12-5827-2012)
313 12-5827-2012

314 Dessler, A and Sherwood, S. (2004). Effect of convection on the summertime extratropical lower
315 stratosphere. *J. Geophys. Res.* 109: D23301. <https://doi.org/10.1029/2004JD005209>

316 Feng, L., and Zhou, T. (2012). Water vapor transport for summer precipitation over the Tibetan Plateau:
317 Multidata set analysis, *J. Geophys. Res.*, 117, D20114, doi:10.1029/2011JD017012

318 Fu, R., Hu, Y., Wright, J., Jiang, J., H., Dickinson, R., E., Chen, M., X., Filipiak, M., Read, W., G., Waters,
319 W., W., and Wu, D., L. (2006). Short circuit of water vapor and polluted air to the global stratosphere
320 by convective transport over the Tibetan Plateau, *Proceedings of the National Academy of Sciences of*
321 *the United States of America*. 103: 5664-5669. <https://doi.org/10.1073/pnas.0601584103>

322 Gao, Y, Cuo, L and Zhang, Y. (2014). Changes in Moisture Flux over the Tibetan Plateau during 1979–
323 2011 and Possible Mechanisms. *J. Climate* ; 27: 1876-1893. [https://doi.org/10.1175/JCLI-D-13-](https://doi.org/10.1175/JCLI-D-13-00321.1)
324 00321.1

325 Garny, H. and Randel, W. J. Transport pathways from the Asian monsoon anticyclone to the stratosphere,
326 *Atmos. Chem. Phys.* (2016); 16: 2703–2718, [https://doi.org/10.5194/acp-16-2703-](https://doi.org/10.5194/acp-16-2703-2016) 2016,.

327 James, R. , Bonazzola, M. , Legras, B. , Surbled, K. , & Fueglistaler, S. . (2008). Water vapor transport and
328 dehydration above convective outflow during Asian monsoon. *Geophys. Res. Lett.* ; 35: L20810.
329 <https://doi.org/10.1029/2008GL035441>

330 [James, P., Stohl, A., Spichtinger, N.: Climatological aspects of the extreme European rainfall of August](#)
331 [2002 and a trajectory method for estimating the associated evaporative source regions. *Nat Hazards*](#)
332 [Earth Syst Sci, 2004, 4, 733 – 746.](#)

- Luo, Y. , Zhang, R. , Qian, W. , Luo, Z. , and Hu, X. . (2011). Intercomparison of deep convection over the tibetan plateau--asian monsoon region and subtropical north america in boreal summer using cloudsat/calipso data. *Journal of Climate*. 24: 2164-2177.
- Randel, W. J. & Jensen, E. J. (2013).Physical processes in the tropical tropopause layer and their roles in a changing climate. *Nat. Geosci* ,6, 169. <https://doi.org/10.1038/ngeo1733>.
- Reale, O., Feudale, L., Turato, B.: Evaporative moisture sources during a sequence of floods in the Mediter-ranean region. *Geophys Res Lett*, 2001, 28, 2085 – 2088.
- Solomon, S., Rosenlof, K. H., Portmann, R. W., Daniel, J. S.,Davis, S. M. , Sanford, T. J. and Plattner, G. K.(2010). Contributions of stratospheric water vapor to decadal changes in the rate of global warming. *Science*, 327: 1219–1223. <https://doi.org/10.1126/science.1182488>
- Su, H, Read, W, Jiang, J. H. , Waters, J. W. , and Fetzer, E. J. . (2006).Enhanced positive water vapor feedback associated with tropical deep convection: New evidence from Aura MLS. *Geophys. Res. Lett.* ; 33. <https://doi.org/10.1029/2005GL025505>
- Stohl, A., Forster, C., Frank, A., et al.: Technical note: The Lagrangian particle dispersion model FLEXPART version 6.2. *Atmos. Chem. Phys.*, 2005, 5, 2461 – 2474.
- Tian, B, Soden, B, Wu, X. (2004). Diurnal cycle of convection, clouds, and water vapor in the tropical upper troposphere: Satellites versus a general circulation model. *J. Geophys. Res. Atmos.*; 27: 2173-2176. <https://doi.org/10.1029/2003JD004117>
- Tian, W. S., Chipperfield, M. and Lü, D. R.(2009) .Impact of increasing stratospheric water vapor on ozone depletion and temperature change. *Adv. Atmos. Sci.* ; 26: 423–437.<https://doi.org/10.1007/s00376-009-0423-3>
- Wang, Y, Zhang, Y, Chiew, F., McVicar, T., R., Zhang, L., Li, H., and Qin , G. (2017). Contrasting runoff trends between dry and wet parts of eastern Tibetan Plateau, *Sci. Rep. U.K.*7: 15458. <https://doi.org/10.1038/s41598-017-15678-x>

357 Xie, F., Zhou, X. ,Li, J. , Chen, Q. , Zhang, J. , Li, Y.,Ding, R. ,Xue, J. and Ma, X. (2018). Effect of the
358 Indo-Pacific Warm Pool on lower stratospheric water vapor and comparison with the effect of the El
359 Niño–Southern Oscillation. *J. Clim.* 31:929–943.

360 Xu, K., Zhong, L., Ma, Y., Zou, M., and Huang Z., (2020). A study on the water vapor transport trend and
361 water vapor source of the Tibetan Plateau. *Theor. Appl. Climatol.*, **140**, 1031–1042,
362 <https://doi.org/10.1007/s00704-020-03142-2>.

363 Xu, X, Zhao, T, Lu C., Guo, Y., Chen, B., Liu, R., Li, Y., and Shi, X. (2014).An important mechanism
364 sustaining the atmospheric "water tower" over the Tibetan Plateau. *Atmos. Chem. Phys.*14: 11287-
365 11295.<https://doi.org/10.5194/acp-14-11287-2014>

366 Xu, X., Lu, C. Shi, X. and Gao, S. (2008). World water tower: An atmospheric perspective, *Geophys. Res.*
367 *Lett.*, 35, L20815. <https://doi.org/10.1029/2008GL035867>

368 Yanai, M. , Esbensen, S. , and Chu, J. H. . (1973). Determination of bulk properties of tropical cloud
369 clusters from large-scale heat and moisture budgets. *Journal of Atmospheric Sciences*, 30(4), 611-
370 627.[https://doi.org/10.1175/1520-0469\(1973\)030<0611:DOBPOT>2.0.CO;2](https://doi.org/10.1175/1520-0469(1973)030<0611:DOBPOT>2.0.CO;2)

371

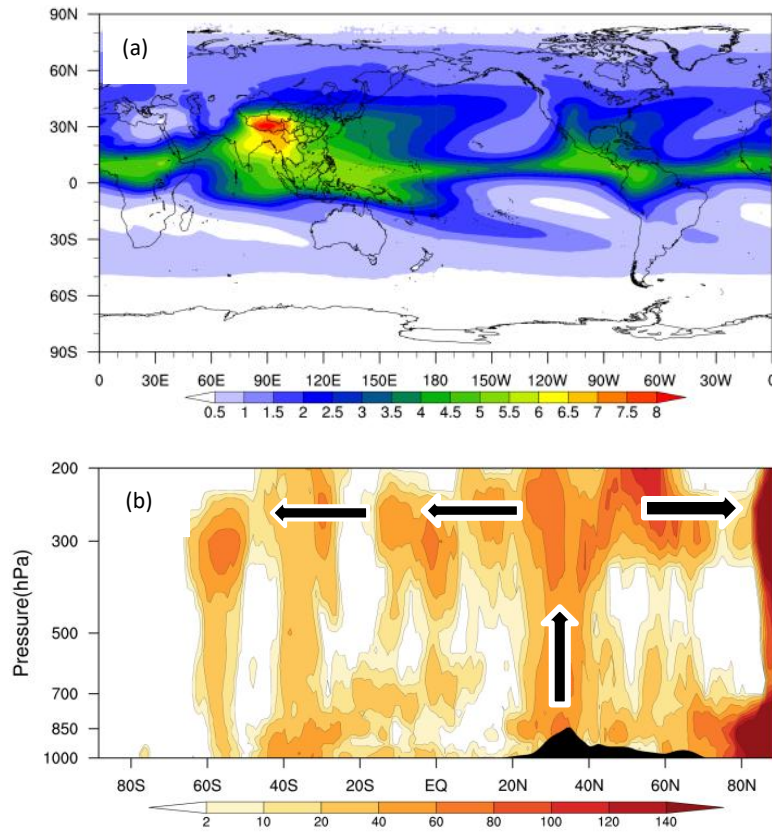


Figure 1.(a) The global distribution of the total water vapor from 300 hPa to 500 hPa based on the summertime AIRS data from 2003 to 2018, (b) the vertical section of the frequency (shaded) of the correlation coefficients passing the level of 90% confidence between summertime TP's low cloud cover and the water vapor at different vertical levels along the meridional direction averaged over 60oE - 180oE for 1979-2016 with the black arrows indicating the connections of TP's low clouds to global water vapor in the upper troposphere with high frequencies.

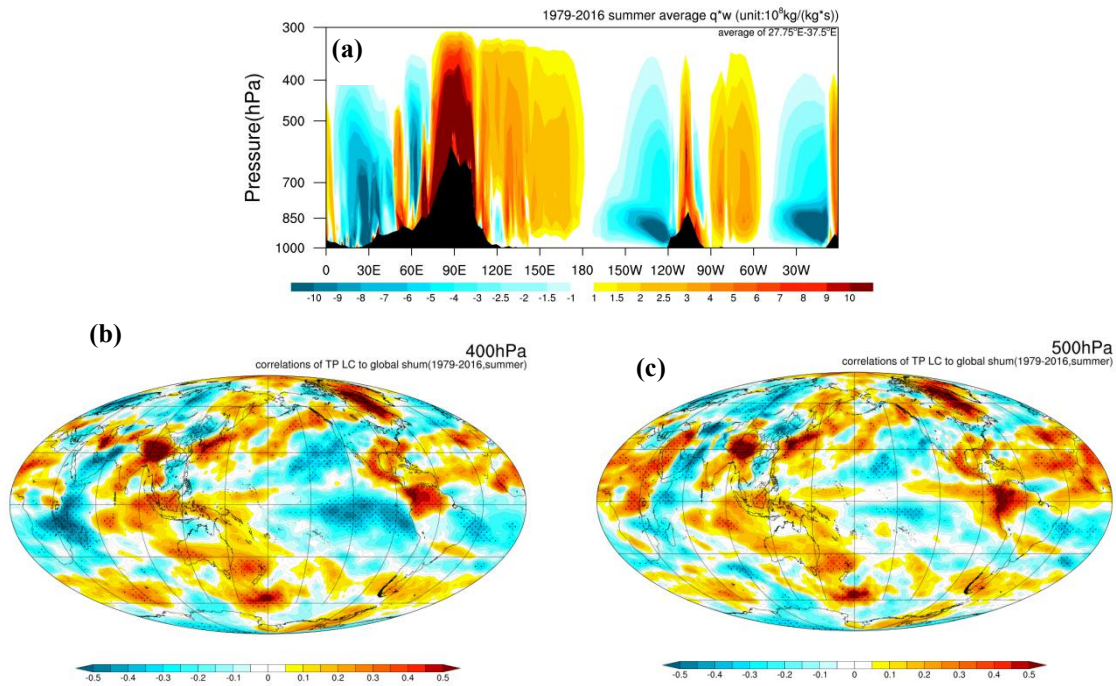


Figure 2 (a) The vertical section of vertical vapor transport flux averaged over 27.5 - 32.0°N in summers of 1979-2016; the spatial distributions of correlation coefficients of low cloud cover over the TP during May, June and July with the global specific humidity of the ECMWF-interim data in Summer (June, July and August) from 1979 to 2018 at (b) 400 hPa and (c) 500 hPa.

420

421

422

423

424

425

426

427

428

429

430

431

432

433

434

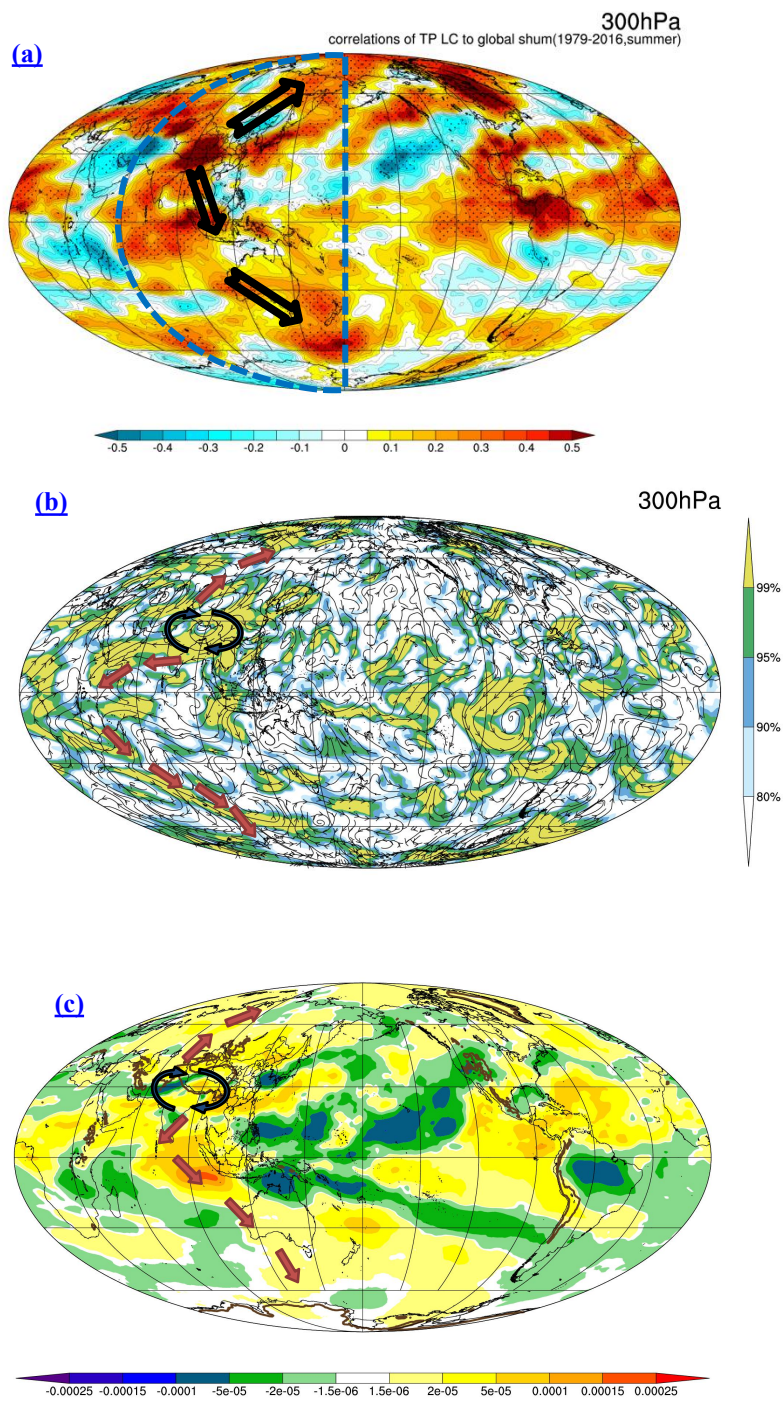
435

436

437

438

439



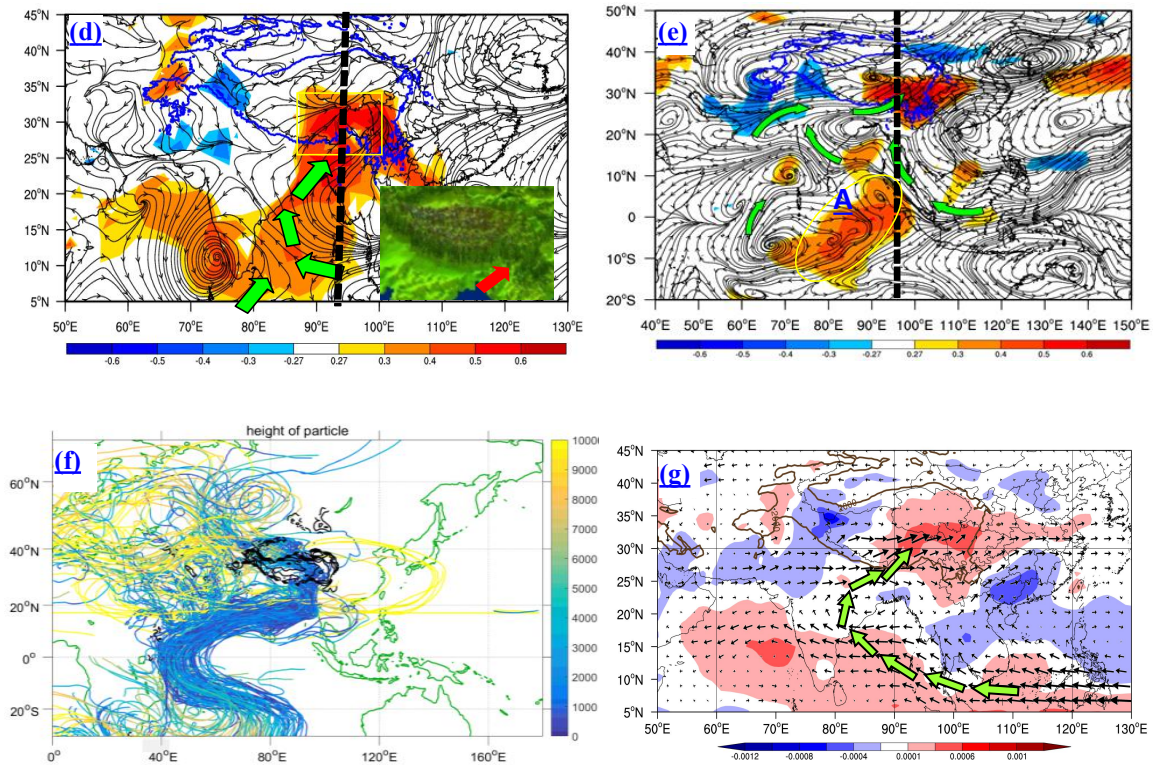


Figure 3. (a) The spatial distributions of correlation coefficients of low cloud cover over the TP with the global specific humidity of the ECMWF-interim data at 300 hPa in summers of 1979-2016 with the pathways of convective air to the troposphere, (b) the fields of correlation vectors (streamlines) of the TP-column Q_1 integrated over the TP region (80-102°E; 30-37.5°N) with the 300hPa vapor transport flux in July of 2014-2016. The shaded area indicates the correlation coefficient passing the 90% confidence level; the water vapor fluxes near the surface layer (the yellow rectangle frame denoting the AWT), (c) the difference of specific humidity (shading, unit: kg/kg) at 300 hPa in summer in 1998 and 2007 with anomalously high Q_1 and in 1997 and 2003 with anomalously low Q_1 in the AWT. The black and orange arrows indicate respectively the anticyclonic circulations in the TP and water vapor transport pathways from the TP to the Arctic and Antarctic regions.; the correlation field

between the total apparent heat source Q_1 over the TP region (80-102°E; 30-37.5°N) with the water vapor (shaded) and water vapor flux (stream lines) in the surface layer (d) and middle layer (500hPa) (e) in summer over 1979-2015, respectively, (f) the backward trajectories of water vapor transport simulated with the model FLEXPART in July, 2009. (g) the difference of vapor transport flux at 500 hPa (vectors, unit: $\text{gs}^{-1}\text{hPa}^{-1}\text{cm}^{-1}$) and specific humidity (color contours, unit: kg/kg) between summers with anomalously high Q_1 in 1998, 2005, 2007, 2008 and 2009 and with anomalously low Q_1 in 1994, 1997, 2001, 2002 and 2003 over the TP

(e) the water vapor fluxes at 500 hPa, (d) correlation vectors of TP-column Q_1 integrated over the TP region (80-102°E; 30-37.5°N) to 300hPa vapor transport flux in July 2014-2016.

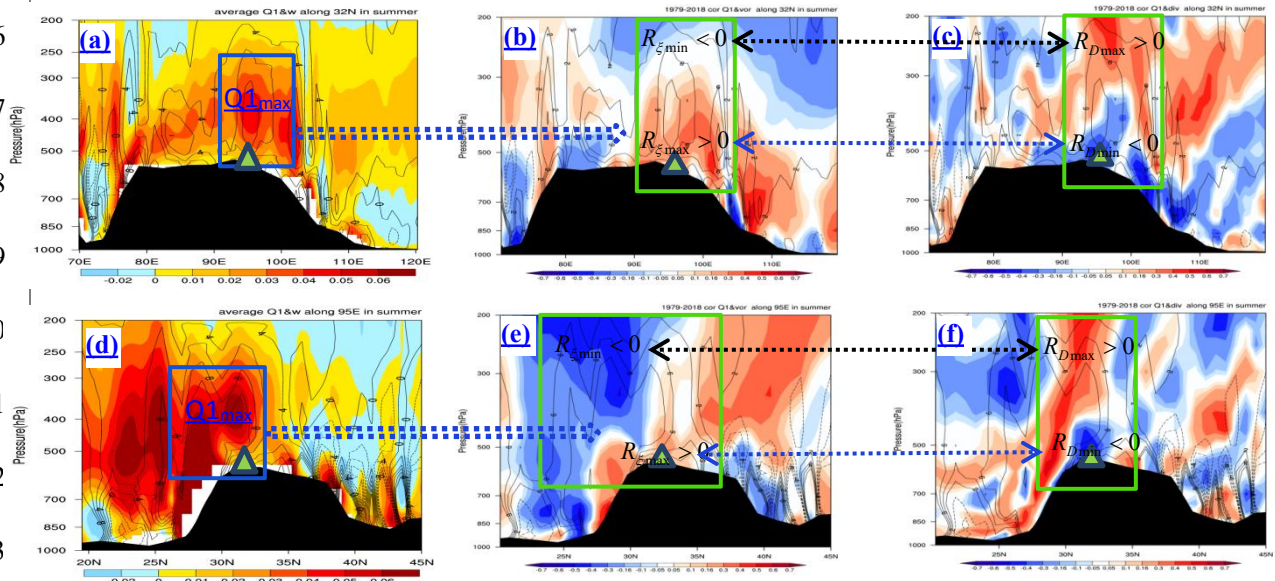


Figure 4. The vertical sections of (a,d) vertical motion (contours, in unit: $10^{-2}\text{Pa}\cdot\text{s}^{-1}$) and column Q_1 (color contours, in unit: 10^{-3}W kg^{-1}); (b,e) The vertical sections of (a) vertical motion (contours, in unit: $10^{-2}\text{Pa}\cdot\text{s}^{-1}$) and (e) correlation coefficients (color

contoursshaded) between Q_1 and the vorticity as well as (c,f) vertical motion (contours, in unit: $10^{-2}\text{Pa}\cdot\text{s}^{-1}$) and the correlation coefficients between Q_1 and the divergence (contours) in the TP, with Figs. a, b and c along 32°N , and Figs. d, e and f along 95°E . The green triangles indicate the AWT core region.

(b, d) separately in the core region of the AWT, in which, a, b is along 32°N , and c, d is along 95°E . The green triangle is the AWT.

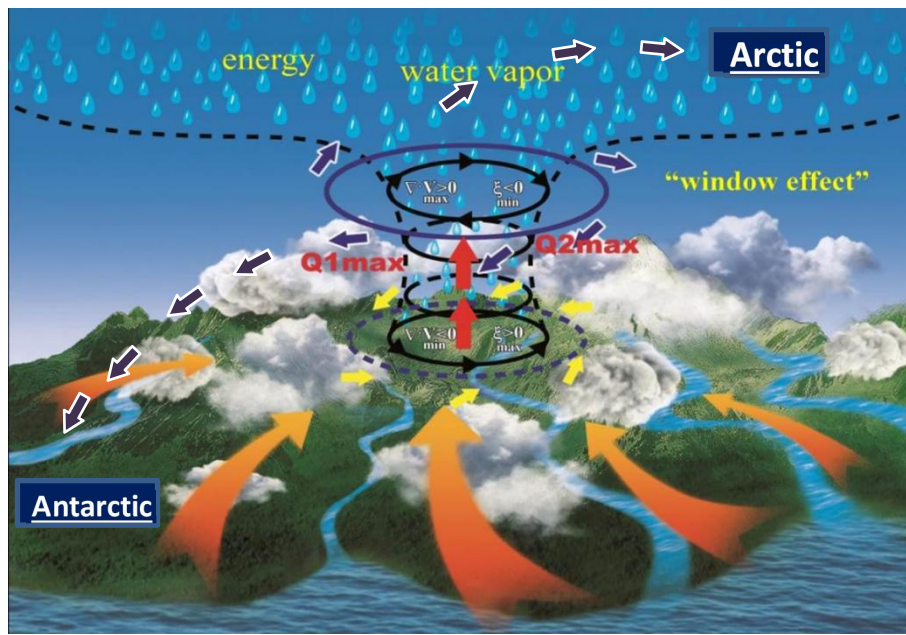


Figure 5. A diagram of vertical water vapor transport in the troposphere driven by the thermal forcing of AWT over the TP, where the vertical transport window of water vapor in the troposphere connects globally the water vapor transport from the tropical oceans

503 and the southern Indian Ocean in the lower troposphere with transport to the Arctic and
504 Antarctic regions in the upper troposphere.

505 ~~**Figure 6.** a diagram of water vapor transport to the troposphere driven by the thermal~~
506 ~~foreing of AWT over the TP.~~